AMERICAN ACADEMY OF OPHTHALMOLOGY®

Genetic Reasons for Phenotypic Diversity in Neuronal Ceroid Lipofuscinoses and High-Resolution Imaging as a Marker of Retinal Disease

Jennifer Huey, LCGC,[1] *Pankhuri Gupta, LCGC,*[2] *Benjamin Wendel, MS,*[1] *Teng Liu, MS,*[1] *Palash Bharadwaj, PhD,*[1] *Hillary Schwartz, BS,*[3] *John P. Kelly, PhD,*[4] *Irene Chang, MD,*[5] *Jennifer R. Chao, MD, PhD,*[1] *Ramkumar Sabesan, PhD,*[1] *Aaron Nagiel, MD, PhD,*[3,6,7] *Debarshi Mustafi, MD, PhD*[1,4,8]

Purpose: To describe the clinical characteristics, natural history, genetic landscape, and phenotypic spectrum of neuronal ceroid lipofuscinosis (NCL)-associated retinal disease.

Design: Multicenter retrospective cohort study complemented by a cross-sectional examination.

Subjects: Twelve pediatric subjects with biallelic variants in 5 NCL-causing genes (CLN3 lysosomal/endosomal transmembrane protein [*CLN3*], CLN6 transmembrane ER protein [*CLN6*], Major facilitator superfamily domain containing 8 [*MFSD8*], Palmitoyl-protein thioesterase 1 ([*PPT1*], and tripeptidyl peptidase 1 [*TPP1*]).

Methods: Review of clinical notes, retinal imaging, electroretinography (ERG), and molecular genetic testing. Two subjects underwent a cross-sectional examination comprising adaptive optics scanning laser ophthalmoscopy imaging of the retina and optoretinography (ORG).

Main Outcome Measures: Clinical/demographic data, multimodal retinal imaging data, electrophysiology parameters, and molecular genetic testing.

Results: Our cohort included a diverse set of subjects with *CLN3*-juvenile NCL (n = 3), *TPP1*-late infantile NCL (n = 5), *PPT1*-late infantile or juvenile NCL (n = 2), *CLN6*-infantile NCL (n = 1), and *CLN7/MFSD8*-late infantile NCL (n = 1). Five novel pathogenic or likely pathogenic variants were identified. Age at presentation ranged from 2 to 16 years old (mean 7.9 years). Subjects presented with varying phenotypes ranging from severe neurocognitive features (n = 8; 67%), including seizures and developmental delays and regressions, to non-syndromic retinal dystrophies (n = 2; 17%). Visual acuities at presentation ranged from light perception to 20/20. In those with recordable ERGs, the traces were electronegative and suggestive of early cone dysfunction. Fundus imaging and OCTs demonstrated outer retinal loss that varied with underlying genotype. High-resolution adaptive optics imaging and functional measures with ORG in 2 subjects with atypical *TPP1*-associated disease revealed significantly different phenotypes of cellular structure and function that could be followed longitudinally.

Conclusions: Our cohort data demonstrates that the underlying genetic variants drive the phenotypic diversity in different forms of NCL. Genetic testing can provide molecular diagnosis and ensure appropriate disease management and support for children and their families. With intravitreal enzyme replacement therapy on the horizon as a potential treatment option for NCL-associated retinal degeneration, precise structural and functional measures will be required to more accurately monitor disease progression. We show that adaptive optics imaging and ORG can be used as highly sensitive methods to track early retinal changes, which can be used to establish eligibility for future therapies and provide metrics for determining the efficacy of interventions on a cellular scale.

Financial Disclosure(s): Proprietary or commercial disclosure may be found in the Footnotes and Disclosures at the end of this article. *Ophthalmology Science 2024;4:100560*

Neuronal ceroid lipofuscinoses (NCLs, CLN, and Batten disease) comprise a group of genetically heterogeneous lysosomal storage disorders that collectively are the most common inherited neurodegenerative disorders of childhood. There are 13 known causative genes, and the mode of inheritance for most is autosomal recessive. All forms of NCL are characterized by the accumulation of autofluorescent storage material in neurons, leading to epileptic seizures, progressive psychomotor retardation, and premature death.[1] In the retina, this abnormal accumulation often leads to generalized photoreceptor disease and profound visual impairment.[2] Neuronal ceroid lipofuscinoses were

https://doi.org/10.1016/j.xops.2024.100560
ISSN 2666-9145/24

historically grouped by age of onset, but because the genetic heterogeneity and the variability of clinical onset, a gene-based nomenclature has been recently adopted.[3] Next generation sequencing technologies have demonstrated that the wide-ranging age of onset and varied retinal disease course in NCL are not only due to the causative gene but more so attributable to specific pathogenic variants. This is best exhibited by *CLN3* disease, which is classically associated with juvenile onset neuronal ceroid lipofuscinosis,[4] whereas certain molecular variants can lead to isolated retinal disease without classic syndromic features.[5,6] Furthermore, classic retinal disease phenotypes in patients with NCL have been associated with complete loss of function for most genes; however, hypomorphic variants can give rise to attenuated disease or distinct phenotypic subtypes of disease. Thus, the understanding of genotype-phenotype correlations for NCLs is important for accurate diagnosis, disease surveillance, and proper management. This is especially true for elucidating the varied effects different genetic variants can have on retinal disease progression.

Salient biomarkers of retinal disease, such as bull's eye maculopathy, are evidenced with fundus autofluorescence,[7] whereas loss of photoreceptors is better visualized with OCT where the integrity of the outer segment layers serve as a surrogate of disease status. However, because of the relatively coarse resolution, these modalities lack the ability to capture subtle cellular-level structural changes. Functional decrements in disease are best identified from electroretinography (ERG),[8] where electronegative ERGs can be seen in patients with NCL.[9] However, a majority of NCL subjects exhibit severely depressed or undetectable ERGs by the time they are evaluated. Furthermore, functional measures such as ERGs, conventional microperimetry, and visual acuity are aggregate and imprecise measures of photoreceptor health that lack spatial resolution; thus, more cellular-scale sensitive measures are required to assess the functional decline.[10] Recently, noninvasive approaches consisting of adaptive optics scanning laser ophthalmoscopy (AOSLO)[11] and optoretinography (ORG)[12] have demonstrated structural and functional characterization of photoreceptors at single cell resolution.[13] The ability to assay the same cellular loci reproducibly over time provides more sensitive measures of disease progression and would provide novel insight into retinal diseases.

In this work, we describe a cohort of 12 subjects with pathogenic or likely pathogenic variants in 5 NCL-causing genes (*CLN3*, *TPP1*, *PPT1*, *CLN6*, and *MFSD8*) that were seen at 2 large tertiary care children's hospitals. This cohort of subjects exhibit a wide range of retinal disease features, including some subjects with seemingly isolated retinal disease and absent (or minimal) extraocular symptoms as well as subjects with classic systemic presentations including seizures, developmental regression, and neurocognitive delays. We report specific genetic variants that are associated with more mild retinal phenotypes. Moreover, we show that adaptive optics-based imaging of subjects with hypomorphic disease variants can reveal cellular-level changes in the retina at different stages of disease and thus provides a more accurate biomarker to monitor disease progression. Overall, this study aims to provide further insight into the phenotypic and genetic spectrum of NCL to better understand retinal manifestations of this complex syndromic disorder.

Methods

Subject Identification and Record Assessment

Patients harboring biallelic pathogenic variants in NCL-associated genes were identified from Seattle Children's Hospital and Children's Hospital Los Angeles. This retrospective study was approved by the institutional review boards at Seattle Children's Hospital and Children's Hospital Los Angeles and adhered to the tenets of the Declaration of Helsinki. Ophthalmic medical records including best-corrected visual acuity (BCVA), slit lamp exam, dilated fundoscopic exam, ERG testing, OCT, and fundus imaging were reviewed. Disease features such as age at symptom onset and age at diagnosis were also noted. Enzyme testing to document deficiencies of PPT1 and TPP1 were reviewed. Molecular genetic testing from Clinical Laboratory Improvement Amendments-certified laboratories for each subject was reviewed as well. Full-field ERG testing was performed using a Ganzfeld bowl and lower eyelid skin electrodes in awake cases or corneal electrodes in anesthetized cases according to protocols adapted from the International Society for Clinical Electrophysiology of Vision standards.[14]

Adaptive Optics Imaging and Optoretinography

Two siblings (subjects 7 and 8) with *TPP1*-associated NCL participated in the cross-sectional component of the study. Tropicamide 1% ophthalmic solution was used for cycloplegia for retinal imaging of both subjects. The research imaging was approved by the University of Washington institutional review board, and all subjects signed an informed consent before their participation and after the nature and possible consequences of the study were explained. All procedures involving human subjects were in accordance with the tenets of the Declaration of Helsinki.

Two different imaging paradigms were used, each aimed at assessing structure and function with high resolution and sensitivity. First, a previously described AOSLO[15] instrument was used to image the central 5 by 2 degrees of temporal retina with image focus set to the photoreceptor layers in order to resolve individual cones. At each eccentricity, 2 to 3 videos of 5 second duration and 1 degree field of view were acquired. These videos were registered to compensate for eye movements and generate a high signal-to-noise ratio image. These images were montaged using an open-source tool.[16] Regions-of-interest of size 100 × 100 μm were selected, and cones were counted in each region of interest for subject 8.

Optoretinography was then conducted with subjects' fixation centered at 2.5 degrees temporal eccentricity, in overlap with the acquired AOSLO montage for subject 8. Optoretinography is a noninvasive imaging paradigm whereby optical changes in the cone outer segment length in response to a light stimulus provides a direct correlate for phototransduction.[13,17,18] The ORG acquisition and analysis paradigm followed previously published procedures[17] using a coarse-scale ORG instrument with OCT volumes spanning 5 by 3 degrees of the retina, acquired using a line-scan OCT[17] after 1 minute of dark-adaptation and a 520-nm stimulus flash. The nominal photon density is based on a nominal eye (24-mm axial length, 7-mm pupil size) of 14.0×10^6 photons/micron^2 and a stimulus duration of 32 ms. The photon density of subject 8 was 18.8×10^6 photons/micron^2, and the age-matched control's photon density was 16.8×10^6 photons/micron^2 after calculations. The subjects' pupil size and axial length, in addition to the stimulus strength at the cornea, were used to calculate stimulus photon density at the retina (photons/square micrometer). Optical phase change in response to

the light stimulus was calculated in the cone outer segment from the difference in phase between the 2 ends of the inner-outer segment function and cone outer segment tips and converted to changes in optical path length (ΔOPL). The variation in ΔOPL was assessed as a function of eccentricity.

Statistical Analysis

Qualitative data such as patient demographics are summarized in tables. For quantitative data assessment, the mean along with error bars calculated from a 95% confidence interval are presented. Differences between control and NCL cone density measurement at a specific eccentricity were assessed with a *t* test and considered significant if *P* values were <0.05. All analyses were performed using R Studio.

Results

Genotypic Determinants of Phenotypic Features of Juvenile *CLN3*-Related NCL

CLN3-associated NCL is the most common and best studied in the context of retinal disease.[4] Three subjects in our cohort harbor pathogenic variants in *CLN3* (Table 1). Two of the subjects (subjects 1 and 2) exhibited typical systemic findings of NCL, such as seizure disorder, whereas the third (subject 3) had isolated retinal disease consistent with retinitis pigmentosa (Fig 1). Subjects 1 and 2 presented for clinical evaluation by age 10 for poor vision, with BCVA measurements in the 20/250 to 20/500 range. Initial examination findings were consistent with a rod-cone dystrophy (Fig 1A). Over the course of follow-up, both had significant visual decline to count fingers/hand motions visual acuity. In contrast, subject 3 presented at age 15 with complaints of nyctalopia with BCVA of 20/25 and constriction of visual fields in both eyes. Ocular exam revealed bone spicule pigmentation and attenuated retinal vessels with OCT imaging indicative of outer retinal atrophy but with foveal sparing (Fig 1B). At the most recent visit, 8 years since the initial diagnosis, subject 3 did not exhibit any syndromic features suggestive of NCL and BCVA and retinal examinations have been stable.

All 3 subjects were found to harbor 2 pathogenic variants in the *CLN3* gene (Table 2). Genetic testing revealed that

Table 1. Clinical Features at Presentation to Ophthalmology

ID#	Age* (Years)	Sex	Gene Affected	Enzymatic Activity	Clinical Exam and Imaging Findings	Snellen VA (OD, OS)	Extraocular Features
1	9	M	*CLN3*	n/a	RPE mottling, hypo- and hyperautofluorescence on FAF, diffuse photoreceptor loss on OCT	20/250, 20/250	Seizures
2	10	F	*CLN3*	n/a	RPE mottling, hypoautofluorescence on FAF, diffuse photoreceptor loss on OCT	8/200, 7/200	Seizures
3	15	F	*CLN3*	n/a	Bone spicule pigmentation	20/25, 20/25	None
4	6	M	*TPP1*	NR	Mild optic disc pallor, mild myopia	LP with "good fixation"	Present, but NR
5	4	F	*TPP1*	~3%	Mild optic disc pallor, perifoveal darkening, pigmentary changes in peripheral retina and along arcades, myopia with astigmatism	20/260, 20/380	Epilepsy, developmental regression
6	3	F	*TPP1*	Absent	Optic disc pallor, bulls eye maculopathy, attenuated vessels, peripheral nonperfusion and atrophy, myopia with astigmatism	Unable to test monocular vision	Seizures, developmental regression including worsening gait and inability to grip food
7	2	M	*TPP1*	5%–9%	RPE mottling, bulls eye maculopathy	20/30, 20/25	Cognitive delays, poor coordination, dyslexia, tremors
8	16	F	*TPP1*	8%–11%	Central macula hyperautofluorescence on FAF	20/20, 20/20	History of failure to thrive, mild neutropenia
9	12	M	*PPT1*	27%	Blunted foveal light reflex, attenuated retinal vessels, retinal atrophy, hyperautofluorescence around fovea	20/80, 20/63	Developmental delay, learning disability, sleep disturbances, microcephaly
10	8	M	*PPT1*	Absent	Few hypopigmented deposits in macula, blunted foveal light reflex, central hypoautofluorescence with surrounding hyperautofluorescence	20/100, LP	None
11	4	M	*CLN6*	n/a	Esotropia, hyperopia, astigmatism, nystagmus	LP with "poor grimace to light"	Present, but NR
12	5	M	*MFSD8*	n/a	Optic disc pallor, blunted foveal light reflex, attenuated vessels, atrophic peripheral retina	20/260, 20/380	Neurocognitive decline, seizures, dysphagia

FAF = fundus autofluorescent imaging; LP = light perception; NR = not reported; OD = right eye; OS = left eye; RPE = retinal pigmented epithelium; VA = visual acuity.
*Age at presentation to ophthalmology for clinical evaluation.

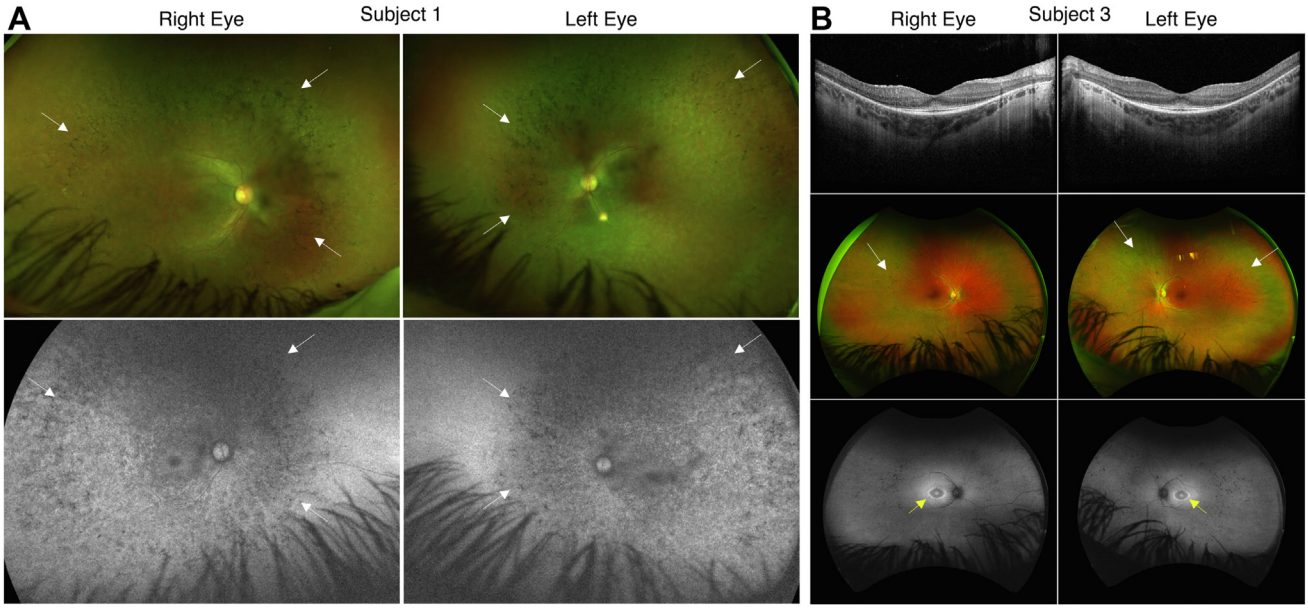

Figure 1. CLN3-related neuronal ceroid lipofuscinoses can exhibit extraocular and isolated retinal findings. **A,** In subject 1 with systemic features of disease, there are extensive bone spicule-like pigmentary changes on fundus imaging with fundus autofluorescence demonstrating widespread hypoautofluoresence (white arrows). In contrast, in (**B**) subject 3 the OCT images demonstrate loss of outer segments with relative foveal preservation with a thickened external limiting membrane. Fundus photos show peripheral bone spicules (white arrows) and fundus autofluorescence shows bulls eye hyperautofluorescence in the macula (yellow arrow).

both subjects 1 and 2 harbored a splice region variant c.125+5G>A in intron 2 of *CLN3*. This variant was homozygous in subject 1 and compound heterozygous in subject 2, occuring in *trans* with a truncating variant, c.597C>A, p.Tyr199*. Genetic testing of subject 3 revealed a heterozygous missense variant, c.1213C>T (p.Arg405Trp) in *trans* with a large deletion encompassing exons 8 and 9 in the CLN3 gene.

Phenotypic Variability of *TPP1*-Related NCL Is Associated With Functional Effects of Disease-Causing Variants

Subjects 4, 5, and 6 were all referred to the ophthalmology clinic by age 6 for decreased visual behavior with extraocular features consistent with NCL. Fundus examination findings of all 3 subjects revealed optic nerve pallor, peripheral retinal pigmentary changes as well as macular pigmentary findings suggestive of bull's eye maculopathy. Electroretinograms were performed in subjects 5 and 6 within 1 year of initial ocular evaluation. Subject 5 had a more severely extinguished ERG recording (Fig 2A) compared to subject 6, but both subjects exhibited reduced b-wave resulting in an electronegative ERG. Because in subject 6 the ERG waveforms were more preserved, it was noted that the electronegative traces were more prominently noticeable under photopic conditions suggestive of early cone dysfunction and their associated bipolar cell pathways. The photopic ERG also demonstrated that, with increasing flash intensities, the a-wave increased, whereas the b-wave was prolonged, further suggesting early involvement of the cone bipolar cells (Fig 2A).

Genetic testing for subject 4 revealed a homozygous pathogenic variant in the *TPP1* gene c.1497delT (p.Gly501Alafs*18) (Table 2), which disrupts a region of the TPP1 protein in which other variant(s) (i.e., p.Trp542*) have been determined to be pathogenic.[19] Subjects 5 and 6 were homozygous for the same splice acceptor variant in the *TPP1* gene (c.509-1G>C), which is one of the most common *TPP1* pathogenic variants worldwide.[21] Follow-up TPP1 enzyme activity analysis in leukocytes revealed low residual TPP1 enzyme activity in subject 5 (~3%) and absent TPP1 enzyme activity in subject 6 (Table 1).

Comparatively, subjects 7 and 8 presented for ophthalmologic evaluation at much later ages (15 and 16 years of age, respectively) with near normal BCVA at initial ophthalmologic evaluation. Subject 7 had onset of neurological symptoms at 2 years of age, including cognitive delays, poor coordination, dyslexia, and tremors and was initially diagnosed with spinocerebellar ataxia 7 because of lack of ocular findings at the time of diagnosis. Worsening visual acuity over time prompted referral to an ophthalmologist at age 15. The initial dilated fundus exam was notable for bull's eye maculopathy in both eyes. Multimodal retinal imaging was further supportive of outer retinal loss in the macula with foveal sparing (Fig 2B, C). Electroretinography recordings of subject 7 revealed normal scotopic traces but mildly subnormal photopic waveforms, amplitudes, and latencies (Fig 2A). These ERG findings were suggestive of early cone photoreceptor dysfunction. In contrast, subject 8, who is the younger sibling of subject 7, did not exhibit any structural retinal disease features at age 15 (Fig 2B, C) with no functional decrements, as evidenced by normal scotopic and photopic ERG traces (Fig 2A).

Table 2. Genetic Testing Results of NCL Cohort Subjects

ID	Gene	Coding Change	Protein Change	GRCh38 (hg38) Coordinates	Classification	Previously Reported Refs
1	*CLN3*	c.125+5G>A		chr16:28491477-C-T	Likely pathogenic	5,6,19,20
2	*CLN3*	c.125+5G>A		chr16:28491477-C-T	Likely pathogenic	5,6,19,20
		c.597C>A	p.Tyr199*	chr16:28486427-G-T	Pathogenic	5,19,20
3	*CLN3*	c.1213C>T	p.Arg405Trp	chr16:28477620-G-A	Pathogenic	5,6,20
		Ex8_9del		chr16:28486650-28486347del†	Pathogenic	5,6
4	*TPP1*	c.1497delT	p.Gly501Alafs*18	chr11:6614920del	Pathogenic	19,21
5	*TPP1*	c.509-1G>C		chr11:6617154-C-G	Pathogenic	21
6	*TPP1*	c.509-1G>C		chr11:6617154-C-G	Pathogenic	21
7	*TPP1*	c.837C>G	p.Tyr279*	chr11:6616710-G-C	Pathogenic	No
		c.508+4A>G		chr11:6617297-T-C	Likely pathogenic	No
8	*TPP1*	c.837C>G	p.Tyr279*	chr11:6616710-G-C	Pathogenic	No
		c.508+4A>G		chr11:6617297-T-C	Likely pathogenic	No
9	*PPT1*	c.236A>G	p.Asp79Gly	chr1:40092171-T-C	Pathogenic	19,22,23
10	*PPT1*	c.29T>A	p.Leu10*	chr1:40097210-A-T	Pathogenic	19,24,25
		c.749G>T	p.Gly250Val	chr1:40076891-C-A	Likely pathogenic	19,22,23
11	*CLN6*	c.247dup	p.Asp83Glyfs*49	chr15:68214340dup	Pathogenic	No
12	*MFSD8*	c.1217_1218dup	p.Trp407Profs*8	chr4:127921656dup	Pathogenic	No
		Ex11_13del		chr4:127921963-127920630del†	Pathogenic	No

NCL = neuronal ceroid lipofuscinoses.
†Approximate based on short-read clinical sequencing.

Subjects 7 and 8 both harbored a heterozygous truncating variant (c.837C>G, p.Tyr279*) and a heterozygous novel intronic variant (c.508+4A>G) in the TPP1 gene, confirmed in *trans* by parental testing. Following genetic testing, TPP1 enzyme activity was used to confirm the pathogenicity of the novel intronic variant,[26] which revealed decreased TPP1 activity at 5% to 9% in dried blood spots forsubject 7 and at 8% to 11% in leukocytes for subject 8.

Genotypic Determinants of Phenotypic Features of Late Infantile *PPT1*-Related NCL

There were 2 subjects in our cohort with *PPT1*-associated disease, which is associated with late infantile neuronal ceroid lipofuscinosis 1 (CLN1) disease.[27] Both had genetically confirmed disease, yet only subject 9 had syndromic features of *PPT1*-associated NCL. Subject 9 had a history of microcephaly at birth, delayed speech, learning and motor milestones at the age of 2 to 3 years and sleep disturbances starting at the age of 8 to 9 years. This subject also had difficulties in school and increasing issues with memory, impulse control, and attention with age. Enzyme activity testing revealed approximately 27% residual PPT1 enzyme activity in leukocytes, which is at the low-end of normal range. At the initial ophthalmology visit, the subject had reduced BCVA and examination findings were consistent with bull's eye maculopathy (Fig 3A). The initial ERG performed under sedation was consistent with generalized photoreceptor dysfunction. Serial OCT scans over a course of a year demonstrated decrease in the ellipsoid zone band width, consistent with worsening disease (Fig 3A). Genetic testing for subject 9 revealed a pathogenic homozygous loss-of-function variant c.236A>G (p.Asp79Gly), which has been reported to cause reduction of palmitoyl-Coenzyme A hydrolase activity by approximately 90%[28] and has been observed in cases of juvenile-onset CLN1 disease.

Subject 10 developed symptoms of bilateral retinal degeneration with cystic macular changes in the right eye without systemic features at presentation at the age of 7 years (Table 1). Enzymatic activity testing of PPT1 on dried blood spots revealed absent enzyme activity. At the time of initial ophthalmology visit, the BCVA was noted to be 20/125 in the right eye with no light perception vision in the left eye. Dilated examination revealed macular dystrophy with bull's eye findings. This was consistent with fundus imaging showing small deposits in the macula with central hypoautofluorescence with surrounding hyperautofluorescence signals in both eyes with fundus autofluorescence imaging (Fig 3B). Serial OCT scans over the course of a year revealed decrease in the ellipsoid zone band width with increased hyperreflective foci (Fig 3B). Electroretinography demonstrated severe rod degeneration and residual cone function in both eyes. At the most recent visit 3 years after initial symptom onset, the subject continued to have a predominantly retinal phenotype with limited neuropsychological deficits in verbal and fluid reasoning and fine motor skills. The subject had no other concerns of coordination issues, tremor, or falls. Genetic testing revealed 1 pathogenic variant c.29T>A (p.Leu10*), which is predicted to cause truncation or nonsense mediated decay of the PPT1 protein,[24] and 1 likely pathogenic variant c.749G>T (p.Gly250Val), which is predicted to lead to a small conformational change that does not affect the active site of the PPT1 protein, thus in theory retaining some enzyme activity.[22]

Genotypic Determinants of Phenotypic Features of *CLN6*-Related NCL

The *CLN6* gene is associated with late-infantile, juvenile, and adult-onset forms of NCL.[29] The presenting feature of many *CLN6*-related NCL cases is motor impairment,

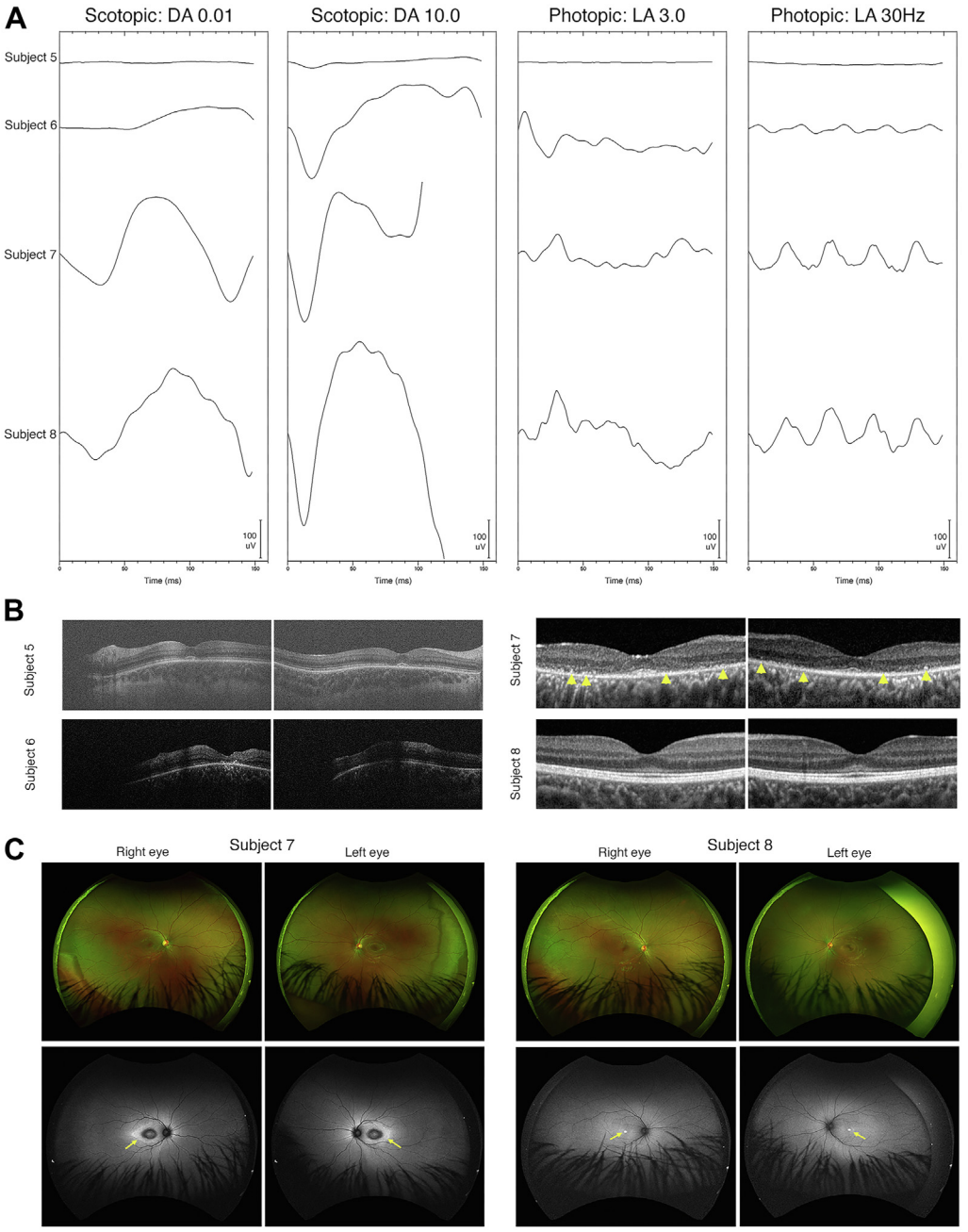

Figure 2. The genotypic determinants of phenotypic features of *TPP1*-related neuronal ceroid lipofuscinoses. **A,** electroretinographys of subjects 5 and 6 demonstrated attenuated traces compared to subjects 7 and 8. In subject 6 there is a characteristic electronegative electroretinography in the photophic traces (light adapted 3.0). In both subjects 6 and 7 there are features of early cone bipolar cell dysfunction with photopic b-wave prolongation. **B,** OCT scans of subjects 5 and 6 were done using a handheld system that shows focal disruption in the fovea. In subject 7 there is patchy loss of the retinal layers with patchy areas of hyperreflective foci (yellow arrowheads) whereas the OCT in subject 8 shows more preserved foveal architecture with lack of hyperreflective foci. **C,** Fundus photos show bull's eye pattern of hyperautofluorescence (yellow arrows) in subject 7 whereas subject 8 has only focal area of hyper autofluorescence at the fovea (yellow arrows).

followed by speech impairment, ataxia, and neurologic deterioration. The visual symptoms for *CLN6*-related NCL, when present, can range from mild signs of retinal degeneration, including optic nerve pallor and vascular thinning, to bull's eye maculopathy or even severe macular and retinal pigment epithelium degeneration.[30]

Subject 11 initially presented to the ophthalmology clinic at 4 years of age with a prior clinical diagnosis of NCL due to systemic symptoms. The BCVA at time of referral was noted as light perception with a poor grimace to light by the referring provider. This subject's visual impairment progressed to no light perception vision by the time of

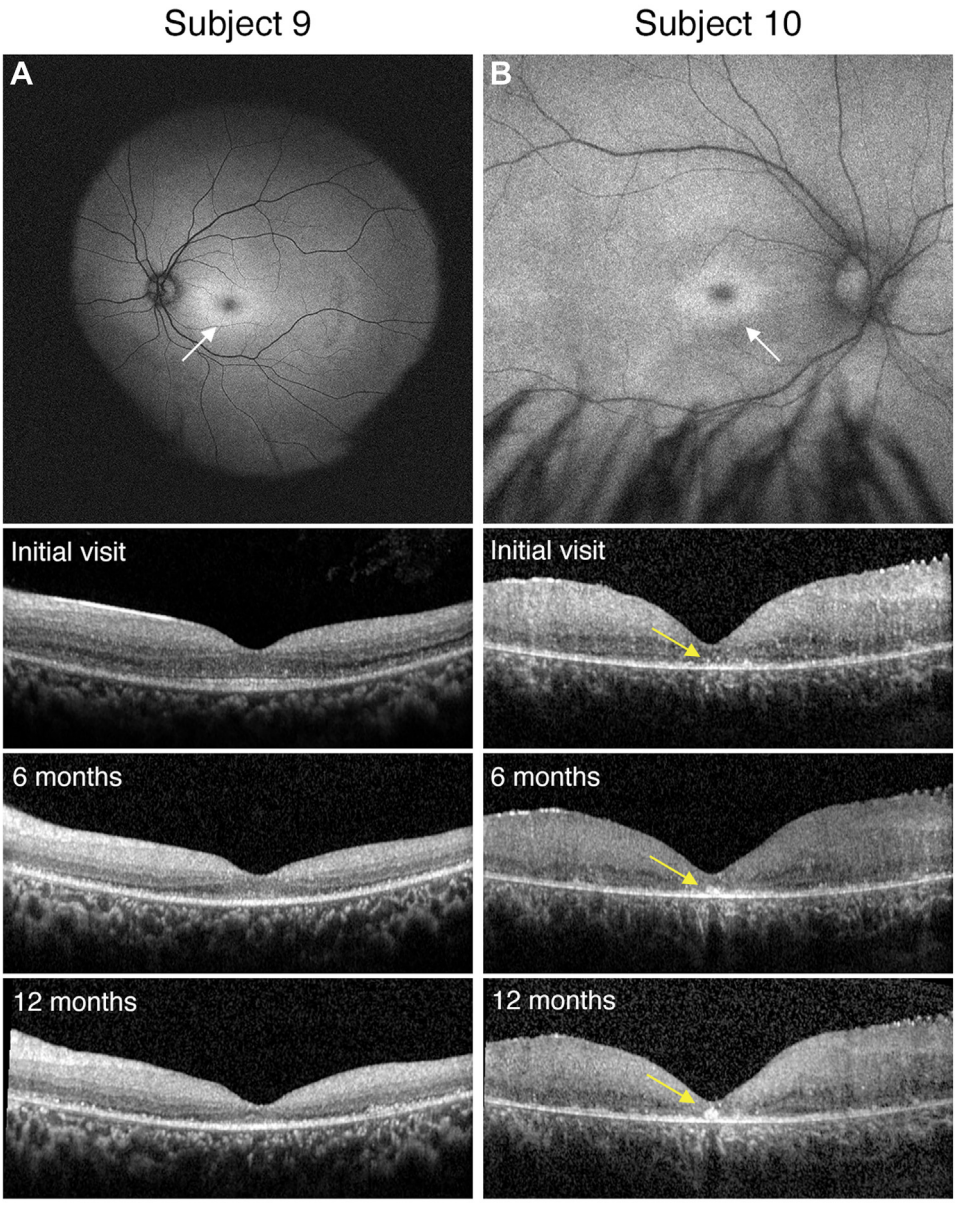

Figure 3. Genotypic variants of *PPT1* can lead to differential retinal phenotypes and progressive features. **A,** In Subject 9 with classic systemic features of neuronal ceroid lipofuscinoses, the exam was consistent with a bulls eye maculopathy as evidenced on fundus autofluorescence (white arrow). Over the course of 1 year follow-up, OCT findings showed progressive loss of the outer retinal layers which correlated with decline in best-corrected visual acuity. **B,** In subject 10 with more isolated retinal findings and genotypic findings consistent with granular osmiophilic deposit, the exam was again consistent with a bulls eye maculopathy as evidenced on fundus autofluorescence (white arrow), but OCT findings were most notable for almost total loss of the outer retinal bands with hyperreflective foci in the fovea that progressively enlarged over the course of 12 months (yellow arrows).

ophthalmology follow-up visit and a thorough dilated fundus examination was challenging, and clinical retinal imaging could not be obtained. Genetic testing for Subject 11 revealed a novel homozygous frameshift variant in *CLN6*, specifically c.247dupG, p.Asp83Glyfs*49. This variant lies in exon 3 of 7, where a number of missense variants, as well as at least one other frameshift variant, have been previously reported as pathogenic,[31] and is absent from large population databases such as gnomAD and ClinVar. In silico analyses predict that this variant is expected to lead to nonsense-mediated decay and loss of gene function.

Genotypic Determinants of Phenotypic Features of Late Infantile *CLN7/MFSD8*-Related NCL

The final patient in our cohort, subject 12, harbored compound heterozygous variants in the *MFSD8* gene, which is associated with a rare subtype termed variant late-infantile neuronal ceroid lipofuscinosis type 7.[32] Subject 12 developed speech impairment, loss of balance, myopic astigmatism, and seizures between the ages of 1 and 5 years, consistent with classic CLN7 presentation.[19,33] The subject was referred to ophthalmology at the age of 5

because of worsening vision, causing the subject to run into objects. At the initial visit, BCVA was 20/260 in both eyes and a dilated fundus examination demonstrated optic disc pallor along with a blunted foveal light reflex, attenuated retinal vessels, and peripheral retinal atrophy in both eyes. These features were also demonstrated on OCT scans. During follow-up visits over the course of 1 year, the patient was noted to have worsened vision and significant neurocognitive decline. An ERG under sedation demonstrated very low to unrecordable traces in both eyes under both scotopic and photopic condition.

Genetic testing for subject 12 revealed 2 pathogenic heterozygous variants in the *MFSD8* gene: a frameshift variant in exon 12 (c.1217_1218dup, p.Trp407Profs*8) and a large deletion encompassing exons 11−13 (Ex11_13del), which are the last 3 exons of the gene. Both of these variants are absent from gnomAD. The *MFSD8* c.1217_1218dup variant (ClinVar ID 1074681) creates a premature translational stop codon in the penultimate exon of the *MFSD8* gene, which is predicted to result in an absent or disrupted protein, which is an established disease mechanism.[19,34] The Ex11_13del variant is absent from ClinVar and is in a region that would disrupt the C-terminus of the protein, where other variants have been shown to be pathogenic.[35]

High-Resolution Imaging Reveals Precise Cellular Level Changes in Disease

The coarse cellular level detail of conventional clinical retinal imaging systems makes it difficult to discern subtle changes with longitudinal imaging. In our cohort we had 2 subjects (subjects 7 and 8 with *TPP1*-related disease) that had relatively mild retinal phenotype without seizures that could comply with high-resolution retinal imaging. Longitudinal clinical imaging of subject 7 over the first year of follow-up revealed no change on clinical examination or multimodal retinal imaging, yet there was reported subjective worsening of visual acuity and functional vision. In comparison, longitudinal clinical imaging of subject 8, who did not report any visual symptoms over the same time span, revealed stable retinal findings as well. To better evaluate more cellular level changes in both subjects, we carried out AOSLO and ORG to more precisely track photoreceptor degeneration.

Although both siblings have the same pathogenic variants in *TPP1*, AOSLO imaging revealed dramatically different structural phenotypes. Subject 7 did not have normal cone structures, as evidenced by a cone mosaic that was severely disrupted with isolated patches of discernible cone reflections (Fig 4B, consistent with photoreceptor degeneration observed on OCT (Fig 4C). In contrast, subject 8 had preserved cone structure in AOSLO and intact outer retinal bands in OCT (Fig 4E, F, respectively) subject 8's variation of cone density versus eccentricity was comparable to normal controls at an age when Subject 7 had already started to exhibit retinal degeneration (Fig 5). Cone density measurements were not possible in subject 7 because of the level of degeneration seen within the cone mosaic. Rather, bright streaks in AOSLO and on the Heidelberg OCT were observed, possibly corresponding to the intracellular accumulation of lysosomal storage material or to reflections from the retinal pigment epithelium and choroid layers (Fig 4B, C).

To understand whether the normal cone structure in subject 7 was consistent with normal function, ORG was acquired in the same retinal area. Optoretinography was unable to reliably be performed for subject 7 because of severe degradation of the photoreceptor outer segment layers. The ORG response is measured as the change in optical path length after stimulus onset, and, in normal controls, this measure increases exponentially before saturating. The same behavior was seen in subject 8's ORG, and her responses were comparable to controls (Fig 6). Both in controls and subject 8, the ORG response decreased with eccentricity in a similar manner, attributable to a decrease in cone OS length. Follow-up course scale ORG of subject 8 done 9 months later at the same retinal locations demonstrated no discernible change in ORG metrics of cone functionality.

Discussion

This report provides new insight into how individual genotypes can influence phenotypic features of retinal disease in different forms of NCL (Table 1). Our cohort included a diverse set of subjects with CLN1, CLN2, CLN3, CLN6, and CLN7 disease. CLN1, CLN2, and CLN3 disease, encoded by the PPT1, TPP1, and CLN3 genes, respectively, are the most common among the pediatric population.[25] Reflecting this disease prevalence, 10 of 12 of our subjects had molecular confirmation of either homozygous or compound heterozygous pathogenic or likely pathogenic variants in PPT1, TPP1, and CLN3. Additionally, 5 novel pathogenic or likely pathogenic variants were identified in this cohort, including *TPP1* c.837C>G (p.Tyr279*), *TPP1* c.508+4A>G, *CLN6* c.247dup (p.Asp83Glyfs*49), *MFSD8* c.1217_1218dup, and *MFSD8* exon 11−13 deletion (Table 2).

Understanding the genetic contributions to disease can have important retinal implications that can help guide the clinician. In certain cases, it may differentiate between a classic, multisystemic NCL presentation and a more isolated retinal phenotype. In CLN3 disease, the second causative variant can determine disease severity. The CLN3 Ex8_9del variant identified in subject 3 is the most common causative variant for CLN3 and is found in >90% of affected individuals.[5] When it is in *trans* with a second severe variant the subject can experience earlier-onset disease with rapid progression,[36] whereas when it is in *trans* with a less severe variant, a milder disease course and even an isolated, nonsyndromic retinal phenotype can be observed.[5] In subject 3, the second variant was a missense variant that is thought to retain some residual functionality resulting in hypomorphic function. Quantitative PCR for a reported patient with the same 2 variants in *CLN3* as Subject 3 (Ex8_9del and p.Arg405Trp) revealed approximately 50% normalized relative quantity of *CLN3* expression compared to wild type.[5] Of note, this reported patient was below the age of 40 at the time of the report and had no extraocular involvement at the time of publication, similar to subject 3.

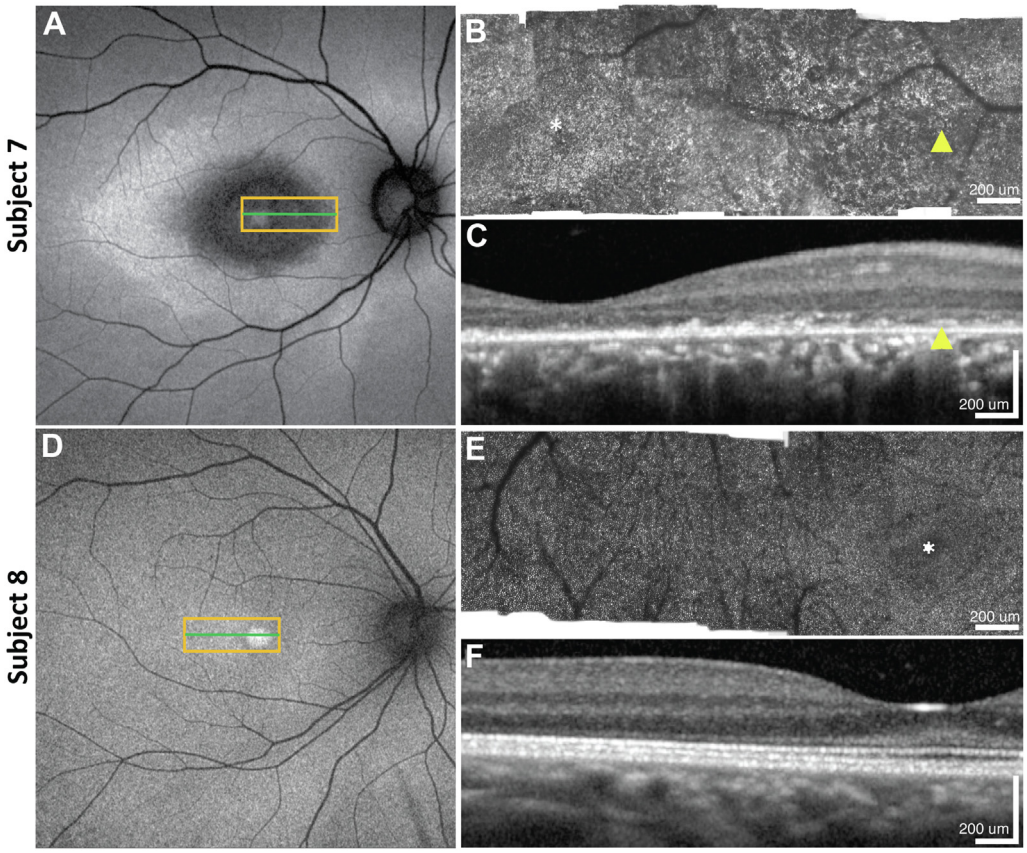

Figure 4. Adaptive optics imaging of siblings with atypical, late-onset *TPP1*-related neuronal ceroid lipofuscinoses. Fundus auto-fluorescence images of subjects 7 and 8, respectively, are shown in panels (**A**) and (**D**) with overlain corresponding adaptive optics scanning laser ophthalmoscopy (AOSLO) (yellow box) and OCT b-scan (green line) locations. Panels (**B**) and (**E**) show AOSLO confocal montage images vertically (foveal center marked with asterisk) aligned to OCT b-scans in panels (**C**) and (**F**), respectively. The streaks of the cone mosaic in AOSLO images of subject 7 in panel **B** correlated to the disrupted outer segment region on OCT (yellow arrowheads). Comparatively, a well ordered cone mosaic on AOSLO in subject 8 corresponds to well preserved outer segments seen on OCT.

Similarly, in those with *PPT1*-associated NCL, the severity of variants and their allelic architecture can dictate the age of onset of potential extraocular features. In those such as subject 10, who harbored a nonsense mutation in *trans* with a missense mutation in the *PPT1* gene, have previously been diagnosed with variant juvenile onset neuronal ceroid lipofuscinosis, also known as granular osmiophilic deposits.[24] Individuals with variant juvenile onset neuronal ceroid lipofuscinosis/granular

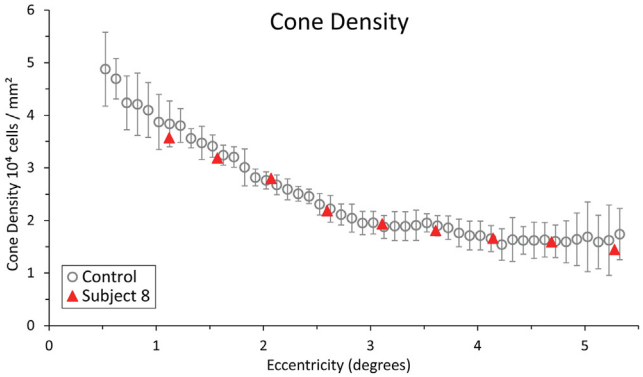

Figure 5. Adaptive optics scanning laser ophthalmoscopy imaging allows for precise cone density measurement in subject 8. Control values (black circles) are a running average of 0.35° bins from 7 control subjects. Error bars are the 95% confidence interval. Each subject 8 data point (red triangles) is from a confocal adaptive optics scanning laser ophthalmoscopy image in the temporal meridian.

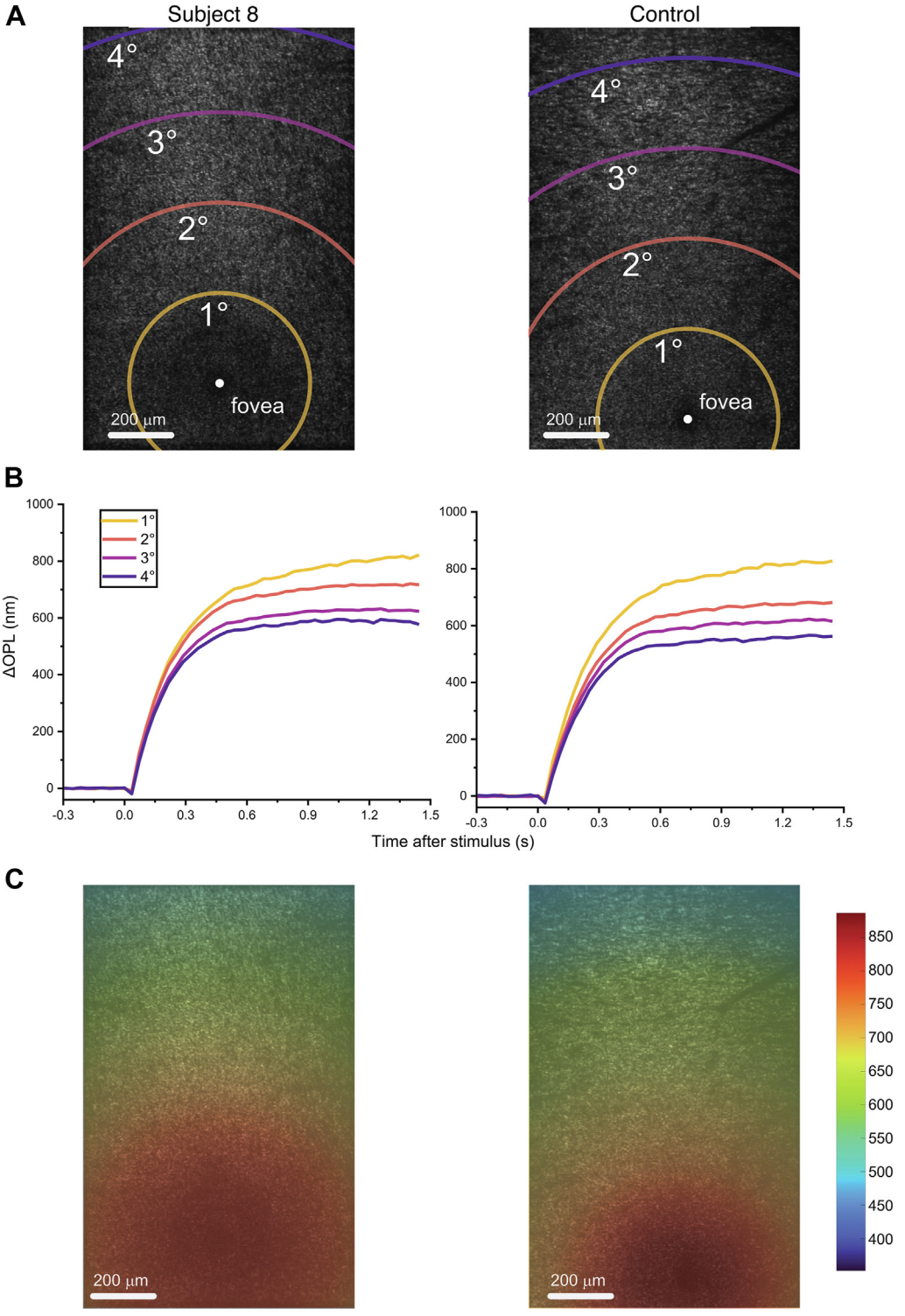

Figure 6. Optoretinography in subject 8 is normal when compared to an age-matched control. **A,** Line-scan OCT volume was segmented to yield an en face image at the inner-outer segment junction (left: subject 8, right: control) annuli indicate eccentricities from fovea to 4 degrees temporal. **B,** optoretinography (ORG) traces for Subject 8 (left) and control (right) showing comparable response kinetics and amplitude across eccentricity. **C,** Structure-function maps, created by combining the OCT structure and ORG function for subject 8 (left) and normal control (right) show a similar trend in ORG response fall-off vs. eccentricity.

osmiophilic deposit show variable phenotypes and can have learning difficulties and seizures in the latter half of the first and second decade respectively, with rapid regression and progression to a vegetative state. Subject 10 was 11 years old at the time of their last visit and, although he did not show any systemic features, there is a possibility they may develop other systemic features at a later age. These 2 cases demonstrate the importance of establishing a genotype-phenotype correlation and highlight the need for close monitoring of potential neurologic symptoms in the future and emphasize the utility of genetic testing in aiding management decisions.

In cases of NCL with systemic findings, gene variant level understanding along with protein level dynamics can provide more accurate insight into disease progression but laboratory findings of enzymatic activity may not always properly predict retinal disease status. Classic *TPP1*-related NCL (CLN2) disease is caused by loss-of-function variants in *TPP1* and is characterized by seizures and delayed language development by 4 years of age[21] followed by a rapid decline in cognitive and motor abilities, with progression of epilepsy and blindness, ultimately leading to death by the first or second decade of life.[37,38] The genetic testing results for subjects 4, 5, and 6 revealed variants that are consistent with the loss-of-function disease mechanism (Table 2). In the case of subjects 5 and 6 who both harbored the same genetic variant, the difference in disease severity highlights that there may be other factors that drive onset and progression. A deeper understanding of protein level dynamics can also explain later onset of symptoms. For example, *CLN3*-related NCL typically presents in early childhood with vision loss between the ages of 4 and 10 years, and progressive behavioral, cognitive, and neurological dysfunction occurring shortly thereafter.[4] Subjects 1 and 2 were found to have the well-known *CLN3* c.125+5G>A variant, which is predicted to alter splicing.[5,6,20] Evidence suggests that mis-spliced transcripts in *CLN3* encode proteins with partial function leading to a milder disease course.[23] This is consistent with the phenotypes observed in subjects 1 and 2 as they both presented to ophthalmology with a suspected rod-cone dystrophy at the ages of 9 and 10 years, respectively, and have minimal neurocognitive symptoms reported to date. Similarly, subject 9 presented with neurological symptoms commonly seen in *PPT1*-related NCL along with low PPT1 enzyme activity. The *PPT1* p.Asp79Gly variant identified in subject 9, despite leading to a large conformational change in the PPT1 protein, has been shown to result in residual enzyme activity.[22]

This work also identified novel disease-causing variants in subjects with clinical features consistent with CLN6 and CLN7 disease. In subject 11, the identified novel frameshift variant (c.247dup, p.Asp83Glyfs*49) resides in exon 3. Previous work has demonstrated that this exon is a mutational hotspot because multiple missense variants, as well as at least one other frameshift variant, have been previously reported as pathogenic[31] and is expected to result in a loss of protein function leading to syndromic disease. In subject 12 with *MFSD8*-associated disease, the identified frameshift variant (c.1217_1218dup, p.Trp407Profs*8) is absent from large population databases but is present in ClinVar and predicted to lead to a loss of gene function due to absent or disrupted protein. The second variant in subject 12 is a large structural variant leading to deletion of exons 11−13, which is also absent from large population databases and is not listed in ClinVar, but it resides in a region that would disrupt the C-terminus of the protein, which is a region where other variants have been shown to be pathogenic.[35] Additionally, large multiexon deletions have been reported in other cases of *MFSD8*-related NCL, such as a large deletion encompassing exons 9 and 10.[39]

Finally, we describe atypical forms of *TPP1*-associated NCL in 2 siblings (subjects 7 and 8). The older sibling, subject 7, was initially diagnosed with spinocerebellar ataxia 7 during adolescence due to lack of retinal issues at that time. It was not until teenage years when retinal signs of disease were first apparent that the diagnostic odyssey was finally narrowed down to NCL. Trio-exome sequencing revealed a likely pathogenic stop gain variant (c.837C>G, p.Tyr279*) in *trans* with a novel intronic variant (c.508+4A>G) in both subjects 7 and 8. Dysfunction of TPP1 leads to accumulation of lysosomal storage material systemically, with neuronal cells like those in the retina particularly susceptible to damage. Because of this effect, those with *TPP1*-associated NCL can have signs of retinal disease as early as 2 years of age and have shortened life-span with death by early adolescence.[40] Thus both subjects 7 and 8 did not fit this phenotypic profile, and we hypothesize that this novel intronic variant is hypomorphic that leads to some residual protein product. The combination of these 2 variants allows for residual TPP1 enzyme activity observed in these subjects and provides a likely explanation why these 2 exhibit more preserved ocular and extraocular functionality into early adulthood.

With the advent of gene replacement and augmentation therapy for retinal diseases, once a diagnosis is confirmed through genetic or enzymatic testing, there is now an emphasized focus on available treatment. For NCLs, there have been great advances in enzyme replacement therapies for *TPP1*-related NCL[41] in which a recombinant human proenzyme of TPP1 is delivered systemically through intracerebroventricular infusions. Whereas this can slow systemic features of disease, it has not been shown to have any effect on the associated retinal disease.[42] Retina-specific therapies for *TTP1*-related NCL are being developed and have been studied in a variety of naturally-occurring animal models (dog, sheep, mice).[43] In fact, a single injection of intravitreal *TPP1* gene therapy in canines before the onset of retinal changes on exam was recently reported to preserve retinal function until the animals reached end-stage neurological disease.[44] The first in human clinical trials in children did not reveal any severe adverse reactions[45]; however, the effectiveness of intravitreal therapy in children was limited because severely affected individuals were first enrolled.[45] In the future it will be imperative to identify the earliest signs of degeneration to enroll those that would benefit the most from intervention.

For new NCL patients, BCVA, slit lamp examination and fundoscopic exam should be routinely performed. In those that are cooperative, clinical imaging consisting of OCT and fundus photography should be attempted. In those that can further tolerate in clinic ERG, it should be collected, and, if not possible, consider an examination under anesthesia. In this cohort, clinical imaging was not available for every subject due to reduced co-operativity in some cases due to neurological disease. Unfortunately, current imaging and functional readouts of retinal health are poor metrics of disease as BCVA may not decrease until cone densities are approximately 40% lower than the average normal eye.[46] Thus, more sensitive methods of retinal imaging and testing are needed in order to intervene at the earliest signs of degeneration. In those that can cooperate further, as subjects 7 and 8 were able to in this study, AOSLO and ORG can be performed to better understand cellular level changes in the retina and better track disease progression longitudinally.

The ORG is a noninvasive sensitive and objective method to measure photoreceptor function. Photoreceptor outer segments are known to change in length in response to visible stimuli. This is attributed to a change in electrical activity and osmotic pressure accompanying the phototransduction cascade.[13,18] The high-resolution images obtained through AOSLO can be used to track structural changes within the cone mosaic of the retina. Therefore, the combination of these modalities can identify early signs of retinal disease, sometimes even before a patient themselves is experiencing changes in their functional vision. In terms of retinal-specific therapies, being able to accurately and repeatedly identify an area of disease will allow clinicians and researchers to better determine the efficacy, if any, of therapeutic interventions.

With the level of sensitivity achieved through both AOSLO and ORG, we are better able to characterize retinal changes not well visualized through standard methods which can provide clinicians with a greater understanding of disease and researchers with clearer targets, such as regions of viable photoreceptors, for therapeutic intervention. A more sensitive measure of photoreceptor functionality against nonretinal manifestations of the genotype provides a holistic picture of disease variants in patients with similar genotypes as well as NCL in general and can more accurately assess treatment responses in the future. In conclusion, the cumulative data from 12 subjects with varying retinal manifestations of NCL highlights the importance of a comprehensive approach in situations where disease genes can give rise to both syndromic and nonsyndromic retinal disease. Advances in genetic testing now allow precise molecular diagnosis to better understand disease progression and potential treatment.

Footnotes and Disclosures

Originally received: February 8, 2024.
Final revision: May 17, 2024.
Accepted: May 23, 2024.
Available online: May 29, 2024. Manuscript no. XOPS-D-24-00042.

[1] Department of Ophthalmology and Roger and Karalis Johnson Retina Center, University of Washington, Seattle, Washington.
[2] Division of Medical Genetics, Department of Medicine, University of Washington, Seattle, Washington.
[3] Department of Surgery, The Vision Center, Children's Hospital Los Angeles, Los Angeles, California.
[4] Division of Ophthalmology, Seattle Children's Hospital, Seattle, Washington.
[5] Division of Medical Genetics, University of California San Francisco, San Francisco, California.
[6] The Saban Research Institute, Children's Hospital Los Angeles, Los Angeles, California.
[7] Department of Ophthalmology, Roski Eye Institute, Keck School of Medicine, University of Southern California, Los Angeles, California.
[8] Brotman Baty Institute for Precision Medicine, Seattle, Washington.

Disclosure(s):
All authors have completed and submitted the ICMJE disclosures form.
The author(s) have made the following disclosure(s):
Supported by National Institutes of Health/NEI (K08EY03378) (A.N.), (K08EY033789) (D.M.), (R01EY029710, U01EY032055) (J.R.C., R.S.), Sinskey Foundation (D.M.), Gerber Foundation (D.M.), Alcon Research Institute (D.M.), Foundation Fighting Blindness (D.M.), Research to Prevent Blindness (A.N., D.M.), Dawn's Light Foundation, and Mark Daily, MD Research Fund (D.M.).
Aaron Nagiel, MD, PhD, an editor of this journal, was recused from the peer-review process of this article and had no access to information regarding its peer-review.

HUMAN SUBJECTS: Human subjects were included in this study. This retrospective study was approved by institutional review boards at Seattle Children's Hospital and Children's Hospital Los Angeles, and adhered to the tenets of the Declaration of Helsinki.

No animal subjects were used in this study.

Author Contributions:

Conception and design: Huey, Gupta, Mustafi

Data collection: Huey, Gupta, Wendel, Liu, Bharadwaj, Schwartz, Kelly, Chang, Chao, Sabesan, Nagiel, Mustafi

Analysis and interpretation: Huey, Gupta, Wendel, Liu, Bharadwaj, Kelly, Chang, Chao, Sabesan, Nagiel, Mustafi

Obtained funding: N/A

Overall responsibility: Huey, Gupta, Sabesan, Nagiel, Mustafi

Abbreviations and Acronyms:
AOSLO = adaptive optics scanning laser ophthalmoscopy; **BCVA** = best corrected visual acuity; **CLN1** = neuronal ceroid lipofuscinosis 1; **ERG** = electroretinography; **NCL** = neuronal ceroid lipofuscinoses; **ORG** = optoretinography.

Keywords:
Adaptive optics, Genetic testing, Juvenile neuronal ceroid lipofuscinosis, Neuronal ceroid lipofuscinoses, Optoretinography.

Correspondence:
Debarshi Mustafi, Department of Ophthalmology and Roger and Karalis Johnson Retina Center, University of Washington, Seattle, WA 98109. E-mail: debarshi@uw.edu.

References

1. Johnson TB, Cain JT, White KA, et al. Therapeutic landscape for Batten disease: current treatments and future prospects. *Nat Rev Neurol*. 2019;15:161−178.
2. Berger W, Kloeckener-Gruissem B, Neidhardt J. The molecular basis of human retinal and vitreoretinal diseases. *Prog Retin Eye Res*. 2010;29:335−375.
3. Williams RE, Mole SE. New nomenclature and classification scheme for the neuronal ceroid lipofuscinoses. *Neurology*. 2012;79:183−191.
4. Wright GA, Georgiou M, Robson AG, et al. Juvenile Batten disease (CLN3): detailed ocular phenotype, novel observations, delayed diagnosis, masquerades, and prospects for therapy. *Ophthalmol Retina*. 2020;4:433−445.
5. Smirnov VM, Nassisi M, Solis Hernandez C, et al. Retinal phenotype of patients with isolated retinal degeneration due to CLN3 pathogenic variants in a French Retinitis Pigmentosa Cohort. *JAMA Ophthalmol*. 2021;139:278−291.
6. Wang F, Wang H, Tuan H-F, et al. Next generation sequencing-based molecular diagnosis of retinitis pigmentosa: identification of a novel genotype-phenotype correlation and clinical refinements. *Hum Genet*. 2014;133:331−345.
7. Kelly JP, Weiss AH, Rowell G, Seigel GM. Autofluorescence and infrared retinal imaging in patients and obligate carriers with neuronal ceroid lipofuscinosis. *Ophthalmic Genet*. 2009;30:190−198.
8. Thompson DA, Handley SE, Henderson RH, et al. An ERG and OCT study of neuronal ceroid lipofuscinosis CLN2 Battens retinopathy. *Eye (Lond)*. 2021;35:2438−2448.
9. Weleber RG. The dystrophic retina in multisystem disorders: the electroretinogram in neuronal ceroid lipofuscinoses. *Eye (Lond)*. 1998;12:580−590.
10. Bensinger E, Rinella N, Saud A, et al. Loss of foveal cone structure precedes loss of visual acuity in patients with rod-cone degeneration. *Invest Ophthalmol Vis Sci*. 2019;60:3187−3196.
11. Wynne N, Carroll J, Duncan JL. Promises and pitfalls of evaluating photoreceptor-based retinal disease with adaptive optics scanning light ophthalmoscopy (AOSLO). *Prog Retin Eye Res*. 2021;83:100920.
12. Lassoued A, Zhang F, Kurokawa K, et al. Cone photoreceptor dysfunction in retinitis pigmentosa revealed by optoretinography. *Proc Natl Acad Sci U S A*. 2021;118:e2107444118.
13. Pandiyan VP, Maloney-Bertelli A, Kuchenbecker JA, et al. The optoretinogram reveals the primary steps of phototransduction in the living human eye. *Sci Adv*. 2020;6:eabc1124.
14. Robson AG, Frishman LJ, Grigg J, et al. ISCEV standard for full-field clinical electroretinography (2022 update). *Doc Ophthalmol*. 2022;144:165−177.
15. Jiang X, Kuchenbecker JA, Touch P, Sabesan R. Measuring and compensating for ocular longitudinal chromatic aberration. *Optica*. 2019;6:981−990.
16. Chen M, Cooper RF, Han GK, et al. Multi-modal automatic montaging of adaptive optics retinal images. *Biomed Opt Express*. 2016;7:4899−4918.
17. Jiang X, Liu T, Pandiyan VP, et al. Coarse-scale optoretinography (CoORG) with extended field-of-view for normative characterization. *Biomed Opt Express*. 2022;13:5989−6002.
18. Pandiyan VP, Nguyen PT, Pugh Jr EN, Sabesan R. Human cone elongation responses can be explained by photoactivated cone opsin and membrane swelling and osmotic response to phosphate produced by RGS9-catalyzed GTPase. *Proc Natl Acad Sci U S A*. 2022;119:e2202485119.
19. Kousi M, Lehesjoki A-E, Mole SE. Update of the mutation spectrum and clinical correlations of over 360 mutations in eight genes that underlie the neuronal ceroid lipofuscinoses. *Hum Mutat*. 2012;33:42−63.
20. Mirza M, Vainshtein A, DiRonza A, et al. The CLN3 gene and protein: what we know. *Mol Genet Genomic Med*. 2019;7:e859.
21. Gardner E, Bailey M, Schulz A, et al. Mutation update: review of TPP1 gene variants associated with neuronal ceroid lipofuscinosis CLN2 disease. *Hum Mutat*. 2019;40:1924−1938.
22. Ohno K, Saito S, Sugawara K, et al. Structural basis of neuronal ceroid lipofuscinosis 1. *Brain Dev*. 2010;32:524−530.
23. Mole SE. The genetic spectrum of human neuronal ceroid-lipofuscinoses. *Brain Pathol*. 2004;14:70−76.
24. Mitchison HM, Hofmann SL, Becerra CH, et al. Mutations in the palmitoyl-protein thioesterase gene (PPT; CLN1) causing juvenile neuronal ceroid lipofuscinosis with granular osmiophilic deposits. *Hum Mol Genet*. 1998;7:291−297.
25. Gardner E, Mole SE. The genetic basis of phenotypic heterogeneity in the neuronal ceroid lipofuscinoses. *Front Neurol*. 2021;12:754045.
26. Mole SE, Anderson G, Band HA, et al. Clinical challenges and future therapeutic approaches for neuronal ceroid lipofuscinosis. *Lancet Neurol*. 2019;18:107−116.
27. Vesa J, Hellsten E, Verkruyse LA, et al. Mutations in the palmitoyl protein thioesterase gene causing infantile neuronal ceroid lipofuscinosis. *Nature*. 1995;376:584−587.
28. Bellizzi 3rd JJ, Widom J, Kemp C, et al. The crystal structure of palmitoyl protein thioesterase 1 and the molecular basis of infantile neuronal ceroid lipofuscinosis. *Proc Natl Acad Sci U S A*. 2000;97:4573−4578.
29. Nicolaou P, Tanteles GA, Votsi C, et al. A novel CLN6 variant associated with juvenile neuronal ceroid lipofuscinosis in patients with absence of visual loss as a presenting feature. *Front Genet*. 2021;12:746101.
30. Badilla-Porras R, Echeverri-McCandless A, Weimer JM, et al. Neuronal Ceroid Lipofuscinosis Type 6 (CLN6) clinical findings and molecular diagnosis: Costa Rica's experience. *Orphanet J Rare Dis*. 2022;17:13.
31. Rus C-M, Weissensteiner T, Pereira C, et al. Clinical and genetic characterization of a cohort of 97 CLN6 patients tested at a single center. *Orphanet J Rare Dis*. 2022;17:179.
32. Brudvig JJ, Weimer JM. CLN7 gene therapy: hope for an ultra-rare condition. *J Clin Invest*. 2022;132:e157820.
33. Topçu M, Tan H, Yalnizoğlu D, et al. Evaluation of 36 patients from Turkey with neuronal ceroid lipofuscinosis: clinical, neurophysiological, neuroradiological and histopathologic studies. *Turk J Pediatr*. 2004;46:1−10.
34. Roosing S, van den Born LI, Sangermano R, et al. Mutations in MFSD8, encoding a lysosomal membrane protein, are associated with nonsyndromic autosomal recessive macular dystrophy. *Ophthalmology*. 2015;122:170−179.
35. Aiello C, Terracciano A, Simonati A, et al. Mutations in MFSD8/CLN7 are a frequent cause of variant-late infantile neuronal ceroid lipofuscinosis. *Hum Mutat*. 2009;30:E530−E540.
36. Mole SE, Zhong NA, Sarpong A, et al. New mutations in the neuronal ceroid lipofuscinosis genes. *Eur J Paediatr Neurol*. 2001;5 Suppl A:7−10.
37. Baranzehi T, Kordi-Tamandani DM, Najafi M, et al. Identification of a TPP1 Q278X mutation in an Iranian patient with

neuronal ceroid lipofuscinosis 2: literature review and mutations update. *J Clin Med Res*. 2022;11:6415.
38. Nickel M, Simonati A, Jacoby D, et al. Disease characteristics and progression in patients with late-infantile neuronal ceroid lipofuscinosis type 2 (CLN2) disease: an observational cohort study. *Lancet Child Adolesc Health*. 2018;2:582–590.
39. Poncet AF, Grunewald O, Vaclavik V, et al. Contribution of whole-genome sequencing and transcript analysis to decipher retinal diseases associated with MFSD8 variants. *Int J Mol Sci*. 2022;23:4294.
40. Steinfeld R, Heim P, von Gregory H, et al. Late infantile neuronal ceroid lipofuscinosis: quantitative description of the clinical course in patients with CLN2 mutations. *Am J Med Genet*. 2002;112:347–354.
41. de Los Reyes E, Lehwald L, Augustine EF, et al. Intracerebroventricular cerliponase alfa for neuronal ceroid lipofuscinosis type 2 disease: clinical practice considerations from US clinics. *Pediatr Neurol*. 2020;110:64–70.
42. Dulz S, Schwering C, Wildner J, et al. Ongoing retinal degeneration despite intraventricular enzyme replacement therapy with cerliponase alfa in late-infantile neuronal ceroid lipofuscinosis type 2 (CLN2 disease). *Br J Ophthalmol*. 2023;107:1478–1483.
43. Murray SJ, Mitchell NL. Ocular therapies for neuronal ceroid lipofuscinoses: more than meets the eye. *Neural Regen Res*. 2022;17:1755–1756.
44. Kick GR, Whiting REH, Ota-Kuroki J, et al. Intravitreal gene therapy preserves retinal function in a canine model of CLN2 neuronal ceroid lipofuscinosis. *Exp Eye Res*. 2023;226:109344.
45. Wawrzynski J, Martinez AR, Thompson DA, et al. First in man study of intravitreal tripeptidyl peptidase 1 for CLN2 retinopathy. *Eye (Lond)*. 2024;38:1176–1182.
46. Foote KG, Loumou P, Griffin S, et al. Relationship between foveal cone structure and visual acuity measured with adaptive optics scanning laser ophthalmoscopy in retinal degeneration. *Invest Ophthalmol Vis Sci*. 2018;59:3385–3393.